# GRAPHICAL STRUCTURE OF ATTRACTION BASINS OF HIDDEN CHAOTIC ATTRACTORS; THE RABINOVICH-FABRIKANT SYSTEM

MARIUS-F. DANCA
*Romanian Institute of Science and Technology,*
*400487 Cluj-Napoca, Romania*
*danca@rist.ro*

PAUL BOURKE
*The University of Western Australia,*
*Crawley, Western Australia, 6009 Australia*
*paul.bourke@uwa.edu.au*

NIKOLAY KUZNETSOV
*Saint-Petersburg State University, St. Petersburg, Russia;*
*Department of Mathematical Information Technology,*
*University of Jyväskylä, Jyväskylä, Finland*
*nkuznetsov239@gmail.com*

Received (to be inserted by publisher)

In the case of systems with hidden attractors and unstable equilibria, the property that hidden attractors are not connected with unstable equilibria is now accepted as one of their main characteristics. To the best of our knowledge this property has not been explored using realtime interactive three-dimensions graphics. Aided by advanced computer graphics analysis, in this paper, we explore this characteristic of a particular nonlinear system with very rich and unusual dynamics, the Rabinovich-Fabrikant system. It is shown that there exists a neighborhood of one of the unstable equilibria within which the initial conditions do not lead to the considered hidden chaotic attractor, but to one of the stable equilibria or are divergent. The trajectories starting from any neighborhood of the other unstable equlibria are attracted either by the stable equilibria, or are divergent.

Keywords: Hidden Chaotic Attractor; Rabinovich-Fabrikant System; Data Visualization

## 1. Introduction

One of the key tasks of the investigation of *dynamical systems* is the study of localization and analysis of *attractors*, i.e. the limited sets of the system states, which are reached by the system from close initial data after transient processes. While trivial attractors, i.e. stable equilibrium points, can be easily revealed analytically or numerically, the search of oscillating periodic or chaotic attractors can turn out to be a challenging problem.

It is easy to visualize and describe the attractor if there is only a single attractor and its basin of attraction is the whole phase space. However the situation becomes complicated when the system is multistable with coexisting attractors [Pisarchik et al., 2014], and some of the attractors are *rare attractors*

with narrow basins of attraction [Zakrzhevsky et al., 2007; Dudkowski et al., 2016]. Various methods for the study of properties of the basin of attraction have been discussed, e.g., in [Brzeski et al., 2017].

For numerical localization of an attractor one needs to choose an initial point in the basin of attraction and observe how the trajectory, starting from this initial point, after a transient process reveals the attractor. Computational errors, caused by a finite precision arithmetic and numerical integration of differential equations, and sensitivity to initial data allow one to get a representative visualization of the *chaotic attractor* by one pseudo-trajectory computed for a sufficiently large time interval. Thus, from a computational point of view, it is natural to suggest the following classification of attractors, based on the simplicity of finding the basins of attraction in the phase space. *Self-excited attractors* can be revealed numerically by the integration of trajectories, started in small neighborhoods of unstable equilibria, while *hidden attractors* have the basins of attraction which are not connected with equilibria and are "hidden somewhere" in the phase space [Leonov et al., 2011; Leonov & Kuznetsov, 2013; Kuznetsov & Leonov, 2014; Leonov et al., 2015; Kuznetsov, 2016].

It should be noted that in the numerical computation of a trajectory over a finite-time interval it is difficult to distinguish a hidden attractor from a *hidden transient chaos* (a transient chaotic set in the phase space, which can persist for a long time) [Danca & Kuznetsov, 2017; Chen et al., 2017; Kuznetsov et al., 2018].[1]

Hidden attractors are attractors in the systems without equilibria (see, e.g. rotating electromechanical systems with Sommerfeld effect (1902) [Sommerfeld, 1902; Kiseleva et al., 2016]), and in the systems with only one stable equilibrium (see, e.g. counterexamples [Leonov & Kuznetsov, 2011, 2013] to Aizerman's (1949) and Kalman's (1957) conjectures on the monostability of nonlinear control systems [Aizerman, 1949; Kalman, 1957]).

One of the first related problems is the second part of 16th Hilbert problem [Hilbert, 1901-1902] on the number and mutual disposition of limit cycles in two dimensional polynomial systems, where nested limit cycles (a special case of multistability and coexistence of periodic attractors) exhibit hidden periodic attractors (see, e.g., [Bautin, 1939; Kuznetsov et al., 2013; Leonov & Kuznetsov, 2013]). The *classification of attractors as being hidden or self-excited* was introduced in connection with the discovery of the first hidden Chua attractor [Kuznetsov et al., 2010; Leonov et al., 2011; Bragin et al., 2011; Leonov et al., 2012; Kuznetsov et al., 2013; Kiseleva et al., 2017; Stankevich et al., 2017] and has captured much attention of scientists from around the world (see, e.g. [Burkin & Khien, 2014; Li & Sprott, 2014; Li et al, 2014; Pham et al., 2014; Chen et al., 2015; Kuznetsov et al., 2015; Saha et al., 2015; Semenov et al., 2015; Sharma et al., 2015; Zhusubaliyev et al., 2015; Wi et al., 2015; Danca et al., 2017; Jafari et al., 2016; Menacer et al., 2016; Ojoniyi & Njah, 2016; Pham et al., 2016; Rocha & Medrano, 2016; Wei et al., 2016; Zelinka, 2016; Borah & Roy, 2017; Brzeski et al., 2017; Feng & Pan, 2017; Jiang , 2016; Kuznetsov et al., 2017; Ma et al., 2017; Messias & Reinol, 2017; Singh & Roy, 2017; Volos et al., 2017; Wei et al., 2017; Zhang et al., 2017]).

For a *self-excited attractor* its basin of attraction is connected with an unstable equilibrium and, therefore, self-excited attractors can be found numerically by the *standard computational procedure* in which after a transient process a trajectory, starting in a neighborhood of an unstable equilibrium, is attracted to the state of oscillation and then traces it; then the computations are performed for a grid of points in the vicinity of the state of oscillation to explore the basin of attraction and improve the visualization of the attractor. Thus, self-excited attractors can be easily visualized (e.g. the classical Lorenz and Hénon attractors are self-excited with respect to all existing equilibria and can be easily visualized by a trajectory from their vicinities).

For a hidden attractor, its basin of attraction is not connected with equilibria and thus the search and visualization of hidden attractors in the phase space may be a challenging task.

In this paper, using advanced graphical tools, we study the neighborhoods of all unstable equilibria in the case of the Rabinovich-Fabrikant system which has five equilibria. For the considered set of parameters, two equilibria are stable, while the other three are unstable. By visualizing the unstable equilibria, one can see that the property of the hidden attractor not being connected with unstable equilibria is confirmed.

[1] Note that generally the transient could have an extremely long lifetime (superpersistent) [Grebogu et al., 1983]. On the other hand, if the time intervals are too large it could lead to inaccurate numerical solutions.

Also, the structure of the attraction basin of the hidden chaotic attractor is unveiled.

## 2. Rabinovich-Fabrikant system

In 1979, Rabinovich and Fabrikant introduced and analyzed from a physical point of view a model of the stochasticity arising from the modulation instability in a non-equilibrium dissipative medium. It is a simplification of a complex nonlinear parabolic equation modelling different physical systems: for the Tollmien-Schlichting waves in hydrodynamic flows, wind waves on water, concentration waves during chemical reactions in a medium in which diffusion occur, Langmuir waves in a plasma etc [Rabinovich & Fabrikant, 1979].

The mathematical model of the Rabinovich-Fabrikant (RF) system is described by the following equations

$$\begin{aligned} \dot{x}_1 &= x_2\left(x_3 - 1 + x_1^2\right) + ax_1, \\ \dot{x}_2 &= x_1\left(3x_3 + 1 - x_1^2\right) + ax_2, \\ \dot{x}_3 &= -2x_3\left(b + x_1x_2\right), \end{aligned} \tag{1}$$

where $a, b > 0$[2]. The nature of the system dynamics is more sensitive to the parameter $b$ than to $a$, as such, $b$ is typically considered as the bifurcation parameter

For $a < b$ we have

$$\operatorname{div}(f(x)) = \sum_{i=1}^{3} \frac{\partial}{\partial x_i} f_i(x) = 2(a-b) < 0.$$

Therefore, the RF system is dissipative in the sense that the flow contracts in volume along trajectories, however it is not dissipative in the sense of Levinson [Leonov et al., 2015], i.e. there is no global bounded convex absorbing set. For example: the Lorenz system has a global bounded convex absorbing set and a global attractor; the classical Henon map has constant negative divergence but is not dissipative in the sense of Levinson and, thus, may have coexisting unbounded trajectories and local attractors with bounded basins of attraction [Kuznetsov et al., 2017]; the system $\ddot{x}_1 + x_1 = 0, \dot{x}_2 = -x_2$ has constant negative divergence $= -1$ but does not have bounded local attractors. Since in the RF system unbounded trajectories can be revealed numerically and there is no global attractor, the search of local hidden attractors is a challenging task.

The system is equivariant with respect to the symmetry

$$T(x_1, x_2, x_3) \to (-x_1, -x_2, x_3). \tag{2}$$

This symmetry means that any orbit, has its symmetrical twin orbit in the sense that all orbits are symmetric one to another with respect to the $x_3$-axis.

Detailed numerical investigations, obtained by taking advantage of increasing computing resources, have been performed for the first time in [Danca & Chen, 2004], and despite the complicated form of the ODEs modeling the system, the RF system has been further numerically studied revealing new interesting aspects. Thus, beside transient chaos, numerically identified heteroclinic orbits[3] and several chaotic attractors with different shapes differentiated by energy-based analysis [Danca et al., 2017], the system exhibits not self-excited chaotic attractors and hidden chaotic attractors but, also chaotic transients [Danca et al., 2016] and hidden chaotic transients [Danca, 2016]. Also the system present multistability [Danca et al., 2016], several different equilibrium states coexisting for a given set of system parameters.

The symmetry (2) is also reflected in the expression of the five equilibrium system's points: $X_0^*(0,0,0)$ and other four points

[2]Negative values also generate interesting dynamics, but this case does not have physical meaning.

[3]Because a complete mathematical analysis to reveal the existence and convergence of heteroclinic is highly problematic, the heteroclinic orbits have been found numerically aided by computer graphic analysis [Danca et al., 2016].

$$X^*_{1,2}\left(\mp\sqrt{\frac{bR_1+2b}{4b-3a}},\pm\sqrt{b\frac{4b-3a}{R_1+2}},\frac{aR_1+R_2}{(4b-3a)R_1+8b-6a}\right),$$
$$X^*_{3,4}\left(\mp\sqrt{\frac{bR_1-2b}{3a-4b}},\pm\sqrt{b\frac{4b-3a}{2-R_1}},\frac{aR_1-R_2}{(4b-3a)R_1-8b+6a}\right),$$

where $R_1=\sqrt{3a^2-4ab+4}$ and $R_2=4ab^2-7a^2b+3a^3+2a$.

One of the two hidden chaotic attractors, $H$ [Danca et al., 2017], is obtained for $a=0.1$ and $b=0.2876$ (Fig. 1).

A relatively large view (with the opposite corners $(-4,-4,0)$, $(0,4,8)$) of the attraction basins of the stable equilibria $X^*_{1,2}$, sliced with the plane $x_1=0$, is presented in Fig. 2 (a) and (b) (blue representing the attractions basin points of the equilibrium $X^*_1$, while green the equilibrium $X^*_2$). The attraction basin of the hidden chaotic attractor $H$ is presented in Fig. 2 (a), (c) and (d). In all images, grey is used to represent the points which generate divergence.

By having five equilibria, the RF system is topological non-equivalent to the classical systems, such as Lorenz and Chen systems (with three equilibria), Rössler system (with two equilibria), some Sprott systems with one equilibrium [Molaie *et al.*, 2013] and so on.

As shown in [Danca et al., 2016], the equilibrium $X^*_0$ is an unstable equilibrium for every $a,b>0$. Furthermore, the line $x_1=x_2=0$, i.e. the $x_3$-axis, is invariant with the reduced equation $\dot{x}_3=-2bx_3$, which has the solution $x_3(t)=e^{-2bt}x_3(0)$. Therefore, all points along $x_3$, which is one-dimensional stable manifold, will be attracted by $X^*_0$, but repulsed along spirals on the two-dimensional unstable manifold $x_3=0$.

To unveil one of the unusual dynamics of this system, for $a=0.1$ and $b=0.2876$, consider initial conditions close to $x_3$ axis (at distance smaller than 0.08 (see Section 3), trajectories will tend, as mentioned before, to one of the stable equilibria $X^*_{1,2}$ (see blue trajectories to $X^*_1$ and red trajectories to $X^*_2$ in Fig. 3 (a) for initial conditions $x_0=(1e-7,1e-7,5)$ and $x_0=(-1e-7,-1e-7,5)$ respectively). This happens, because points situated at distance smaller than about 0.08 belong to one of attraction basins of $X^*_{1,2}$. However, for relative larger values $x_3(0)$ and $x_{1,2}(0)$ but still close to the axis $x_3$, trajectories are no longer attracted by $X^*_{1,2}$ but, after unstable transient oscillations tend to $\pm\infty$ along directions parallel to the axis $x_2$ (see Fig. 3 (b) where $x_0=(1e-7,1e-7,50)$ and $x_0=(-1e-7,-1e-7,50)$ respectively). Similar dynamics appear after some chaotic transient oscillations, which last for a relatively short time integration of about $t\in[0,20]$, for initial conditions on the plane $x_3=0$. Also, there exist divergent trajectories which are first attracted along directions parallel to the axis $x_2$, by some"virtual" saddles, situated at large distances from unstable equilibria $X^*_{3,4}$), this kind of virtual points being presented in [Danca et al., 2016].

For the considered parameters, $a=0.1$ and $b=0.2876$, the equilibria $X^*_{1,2}$ are stable, while $X^*_0$ and $X_{3,4}$ are unstable.

Note that the considered hidden chaotic attractor $H$, coexists with three unstable equilibria [Danca et al., 2017] (see also Fig. 1).

## 3. Graphic analysis

As outlined in the Introduction, an attractor is called a hidden attractor if its basin of attraction does not intersect with small neighborhoods of equilibria. Therefore, to verify that a chaotic attractor of RF's system is hidden, we might numerically check the trajectories starting from initial points situated in small vicinities of unstable equilibria. If there exist such neighborhoods whose points are either attracted by the stable equilibria or are divergent and do not lead to the attractor, then the attractor is considered as being hidden.

Generally, hidden chaotic attractors are found by searching thousands or tens of thousands of initial conditions in the neighborhoods of unstable equilibria, to see whether or not these neighborhoods lead to hidden attractors. This paper presents effective graphical visualizations that are both 3D and interactive of these neighborhoods and of the attraction basins of the one of the hidden chaotic attractors in the case of the RF system.

Consider the hidden attractor $H$ presented in Fig. 1. In order to explore the attraction basin of $H$, parallelepipedic neighborhoods of unstable points have been considered. The points within these neighborhoods will be represented by small spheres. The intensive simulations, lead to a compromise between the computer time and accuracy of the graphical results. Thus, the fixed step of the parallelepiped scanning along the three axes is $1e-3$, or smaller and the size of the sphere radius is scaled so that nearby points (consecutive points, from the scanning point of view) are tangent spheres.

Exploring and understanding the nature of the basin of attraction given the large number of three-dimensional points resulting from the simulations is challenging. One goal was to be able to create representations that could be studied interactively 3D rather than only from fixed viewpoints or only in 2D sections. Another desirable, and often conflicting aim was to subsequently be able to create high quality graphical representations for publication. These goals were met by separating the visualization software from the simulation software. Customized tools were developed for the data visualization aspects of the research, this software creates simplified geometry for realtime exploration and at the same time high quality geometry for ray-traced style rendering. In both cases points were represented by small glyphs, typically spheres or boxes centered on each simulation point and scaled to typically touch the neighboring points. Each point is classified by the attractor it belongs to, this allows the various basins of attraction to be shown individually or all together.

*Remark 3.1.* Different dedicated numerical methods for ODEs, implemented in different software packages, might give different results for the same parameters values and initial conditions. In this paper we utilized the Matlab integrator ode45 with $RelTol = 1e-6$, and $AbsTol = 1e-9$[4] and the integration time $t \in [0, 400]$. In order to have reliable numerical simulations, one has to find a compromise between the relative short time intervals where precise solutions can be found numerically (see e.g. [Sarra & Meador, 2011; Wang et al., 2012]) and the minimum time intervals required to reveal the nature of the systems, and avoid if necessary, the potential chaotic transients. Therefore, the results obtained in this paper are strongly related to the choice and setting up of the numerical method used to integrate this particular system.

Let first consider the unstable equilibrium $X_0^*$. The explored domain, a zoomed parallelepipedic detail from Fig. 2 (a), with opposite corners $(-2,-2,-2)$, $(2,2,1)$, contains $2,000,000$ points so that it includes the hidden attractor $H$ (see Fig.4 (a)). This large number of points determines a sufficiently accurate graphical analysis of the neighborhoods of unstable equilibria.

As shown in Fig. 2 (a), the points considered as initial points of the numerical integration of the system which lead to $X_1^*$ are colored blue (Fig. 5 (a)), those leading to $X_2^*$ in green (Fig. 5 (b)), and points of the attraction basin of the hidden attractor, in red (Fig. 5 (c)). Divergency points (plane $x_3 = 0$) are not shown.

It can be seen that the hidden attractor $H$ evolves along the frontiers of attraction basins of the two stable equilibria (blue and green), where there are a mixed (possible a fractal set) of points attracted by $X_1^*$ and $X_2^*$ (see Fig. 4 (b)). Moreover, these frontiers also contains initial points of $H$.

Even at first sight the origin seems to be surrounded by initial red points which lead to $H$, the "closest" horizontal section to the plane $x_3 = 0$ (Fig. 5 (d)), unveils that one can find an empty disc-like region without red points, of radius of about 0.08, in concordance with the property of hidden chaotic attractors. By the "closest" horizontal plane one understands here the first scanned plane which, in this case, is situated at a distance $x_3 = 0.0001$ from the plane $x_3 = 0$. One can suppose that this region exists also for $x_3 \to 0$.

A zoomed three-dimensional detail of the neighborhood of unstable equilibrium $X_0^*$, beside the possible fractal structure (Fig. 6 (a)), reveals the fact that the "empty-red" region persists along the $x_3$ axis, having a cylinder-like shape (Fig. 6 (b) and (c)). In other words, all initial points within this "empty-red" region lead, by integration, to one of the stable equilibria, $X_1^*$ (blue points) or $X_2^*$ (green points), or are divergent

[4]In [Brenan et al., 1996] the following relative tolerance is proposed: $RelTol = 10^{(m+1)}$, where $m$ is the precise number of digits.

(if the points are on the plane $x_3 = 0$) and not attracted by $H$. Another horizontal section with the plane $x_3 = 0.04$ is presented in Fig. 6 (d) and, compared with that in Fig. 5 (c), indicates that the shape of the boundary of the empty region changes slightly with the variations of $x_3$, but has the same radius size of about 0.08 (Fig. 6 (d)).

Consider now the unstable equilibria $X^*_{3,4}$, as shown in Fig. 7. As can be seen, these equilibria are not related to $H$. The trajectories starting from any neighborhood of these equilibria are attracted either by $X^*_1$ (blue points and trajectories) or by $X^*_2$ (green points an trajectories), or tend to infinity (grey points and trajectories).

Summarizing, all unstable equilibria of the RF system are not connected with $H$. In other words, $H$ cannot be found by starting from initial points of however small neighborhoods of unstable equilibria, such as for self-excited attractors and the largest neighborhood of $X^*_0$, which has no connection with the attraction basin of the hidden attractor $H$ has a well defined unbounded cylinder-like shape. Moreover, for this system the attraction basin of $H$ seems unbounded (see also Fig. 2 (a)).

## Conclusion

In this paper, for the case of the RF system and aided by advanced computer graphic techniques, we visualized both the attraction basins of the stable equilibria and the attraction basin of the considered hidden chaotic attractor. We illustrated that the attraction basin of the hidden chaotic attractor is not connected with unstable equilibria. Also, it is shown that one of the unstable equilibria is connected with the attraction basin of the hidden chaotic attractor, only outside an unbounded cylinder-like neighborhood of the unstable equilibria.

Interactive versions of the 3D figures can be found online at the following address
https://sketchfab.com/pbourke/collections/hidden-attractors
Alternatively, 3D models in the OBJ format can be downloaded from here
http://paulbourke.net/papers/hidden-attractors
OBJ models can be opened in a wide range of 3D viewing software packages.

## Acknowledgements

The work is done within the Russian Science Foundation project (14-21-00041)

## References

Luo, X., Small, M., Danca, M.-F. & Chen G. [2007] "On a dynamical system with multiple chaotic attractors," *Int. J. Bifurcation and Chaos* **17**, 3235–3251.

Danca, M.-F. & Chen, G. [2004] "Bifurcation and chaos in a complex model of dissipative medium," *Int. J. Bifurcation and Chaos* **14**, 3409–3447.

Danca, M.-F, Kuznetsov, K. [2017] "Parameter Switching Synchronization," Applied Mathematics and Computation, 313, 94-102.

Danca, M.-F., Kuznetsov, N., Chen, G. [2017] "Unusual dynamics and hidden attractors of the Rabinovich-Fabrikant system," Nonlinear Dynamics, 88, 1, 791805

Danca, M.-F., Feckan, M., Kuznetsov, K., Chen, G. [2016] "Looking more closely to the Rabinovich-Fabrikant system," International Journal of Bifurcation and Chaos, 26(2), 1650038.

Danca, M.-F. [2016] "Hidden transient chaotic attractors of Rabinovich-Fabrikant system," Nonlinear Dynamics, 86(2), 12631270.

Pisarchik, A.N., Feudel, U.[2014]: Control of multistability. Physics Reports **540**(4) 167–218

Zakrzhevsky, M., Schukin, I., Yevstignejev, V.[2007] Scientific Proc. Riga Technical Univ. Transp. Engin. **6** 79

Dudkowski, D., Jafari, S., Kapitaniak, T., Kuznetsov, N., Leonov, G., Prasad, A.[2016]: Hidden attractors in dynamical systems. Physics Reports **637** 1–50

Brzeski, P., Wojewoda, J., Kapitaniak, T., Kurths, J., Perlikowski, P.[2017]: Sample-based approach can

outperform the classical dynamical analysis - experimental confirmation of the basin stability method. Scientific Reports **7** art. num. 6121.

Leonov, G., Kuznetsov, N., Vagaitsev, V.[2011]: Localization of hidden Chua's attractors. Physics Letters A **375**(23) 2230–2233

Leonov, G., Kuznetsov, N.[2013]: Hidden attractors in dynamical systems. From hidden oscillations in Hilbert-Kolmogorov, Aizerman, and Kalman problems to hidden chaotic attractors in Chua circuits. International Journal of Bifurcation and Chaos **23**(1) art. no. 1330002.

Kuznetsov, N., Leonov, G.[2014]: Hidden attractors in dynamical systems: systems with no equilibria, multistability and coexisting attractors. IFAC Proceedings Volumes **47** 5445–5454

Leonov, G., Kuznetsov, N., Mokaev, T.[2015]: Homoclinic orbits, and self-excited and hidden attractors in a Lorenz-like system describing convective fluid motion. Eur. Phys. J. Special Topics **224**(8) 1421–1458

Kuznetsov, N.[2016]: Hidden attractors in fundamental problems and engineering models. A short survey. Lecture Notes in Electrical Engineering **371** 13–25 (Plenary lecture at International Conference on Advanced Engineering Theory and Applications 2015).

Danca, M.F., Kuznetsov, N.[2017]: Hidden chaotic sets in a Hopfield neural system. Chaos, Solitons & Fractals **103** 144–150

Chen, G., Kuznetsov, N., Leonov, G., Mokaev, T.[2017]: Hidden attractors on one path: Glukhovsky-Dolzhansky, Lorenz, and Rabinovich systems. International Journal of Bifurcation and Chaos **27**(8) art. num. 1750115.

Kuznetsov, N., Leonov, G., Mokaev, T., Prasad, A., Shrimali, M.[2018]: Finite-time Lyapunov dimension and hidden attractor of the Rabinovich system. Nonlinear Dynamics **92**(2) 267–285

Sommerfeld, A.[1902]: Beitrage zum dynamischen ausbau der festigkeitslehre. Zeitschrift des Vereins deutscher Ingenieure (in German) **46** 391–394

Kiseleva, M., Kuznetsov, N., Leonov, G.[2016]: Hidden attractors in electromechanical systems with and without equilibria. IFAC-PapersOnLine **49**(14) 51–55

Leonov, G., Kuznetsov, N.[2011]: Algorithms for searching for hidden oscillations in the Aizerman and Kalman problems. Doklady Mathematics **84**(1) 475–481

Aizerman, M.A.[1949]: On a problem concerning the stability in the large of dynamical systems. Uspekhi Mat. Nauk (in Russian) **4** 187–188

Kalman, R.E.[1957]: Physical and mathematical mechanisms of instability in nonlinear automatic control systems. Transactions of ASME **79**(3) 553–566

Hilbert, D.[1901-1902] Mathematical problems. Bull. Amer. Math. Soc. (8) 437–479

Bautin, N.N.[1939]: On the number of limit cycles generated on varying the coefficients from a focus or centre type equilibrium state. Doklady Akademii Nauk SSSR (in Russian) **24**(7) 668–671

Kuznetsov, N., Kuznetsova, O., Leonov, G.[2013]: Visualization of four normal size limit cycles in two-dimensional polynomial quadratic system. Differential equations and dynamical systems **21**(1-2) 29–34

Kuznetsov, N., Leonov, G., Vagaitsev, V.[2010]: Analytical-numerical method for attractor localization of generalized Chua's system. IFAC Proceedings Volumes **43**(11) 29–33

Bragin, V., Vagaitsev, V., Kuznetsov, N., Leonov, G.[2011]: Algorithms for finding hidden oscillations in nonlinear systems. The Aizerman and Kalman conjectures and Chua's circuits. Journal of Computer and Systems Sciences International **50**(4) 511–543

Leonov, G., Kuznetsov, N., Vagaitsev, V.[2012]: Hidden attractor in smooth Chua systems. Physica D: Nonlinear Phenomena **241**(18) 1482–1486

Kuznetsov, N., Kuznetsova, O., Leonov, G., Vagaitsev, V.[2013]: Analytical-numerical localization of hidden attractor in electrical Chua's circuit. Lecture Notes in Electrical Engineering **174**(4) 149–158

Kiseleva, M., Kudryashova, E., Kuznetsov, N., Kuznetsova, O., Leonov, G., Yuldashev, M., Yuldashev, R.[2017]: Hidden and self-excited attractors in Chua circuit: synchronization and SPICE simulation. International Journal of Parallel, Emergent and Distributed Systems https://doi.org/10.1080/17445760.2017.1334776.

Stankevich, N., Kuznetsov, N., Leonov, G., Chua, L.[2017]: Scenario of the birth of hidden attractors in the Chua circuit. International Journal of Bifurcation and Chaos **27**(12) art. num. 1730038.

Burkin, I., Khien, N.[2014]: Analytical-numerical methods of finding hidden oscillations in multidimensional dynamical systems. Differential Equations **50**(13) 1695–1717

Li, C., Sprott, J.[2014]: Coexisting hidden attractors in a 4-D simplified Lorenz system. International Journal of Bifurcation and Chaos **24**(03) art. num. 1450034.

Li, Q., Zeng, H., Yang, X.S.[2014]: On hidden twin attractors and bifurcation in the Chua's circuit. Nonlinear Dynamics **77**(1-2) 255–266

Pham, V.T., Rahma, F., Frasca, M., Fortuna, L.[2014]: Dynamics and synchronization of a novel hyperchaotic system without equilibrium. International Journal of Bifurcation and Chaos **24**(06) art. num. 1450087.

Chen, M., Li, M., Yu, Q., Bao, B., Xu, Q., Wang, J.[2015]: Dynamics of self-excited attractors and hidden attractors in generalized memristor-based Chua's circuit. Nonlinear Dynamics **81** 215–226

Kuznetsov, A., Kuznetsov, S., Mosekilde, E., Stankevich, N.[2015]: Co-existing hidden attractors in a radio-physical oscillator system. Journal of Physics A: Mathematical and Theoretical **48** 125101

Saha, P., Saha, D., Ray, A., Chowdhury, A.[2015]: Memristive non-linear system and hidden attractor. European Physical Journal: Special Topics **224**(8) 1563–1574

Semenov, V., Korneev, I., Arinushkin, P., Strelkova, G., Vadivasova, T., Anishchenko, V.[2015]: Numerical and experimental studies of attractors in memristor-based Chua's oscillator with a line of equilibria. Noise-induced effects. European Physical Journal: Special Topics **224**(8) 1553–1561

Sharma, P., Shrimali, M., Prasad, A., Kuznetsov, N., Leonov, G.[2015]: Control of multistability in hidden attractors. Eur. Phys. J. Special Topics **224**(8) 1485–1491

Zhusubaliyev, Z., Mosekilde, E., Churilov, A., Medvedev, A.[2015]: Multistability and hidden attractors in an impulsive Goodwin oscillator with time delay. European Physical Journal: Special Topics **224**(8) 1519–1539

Wei, Z., Yu, P., Zhang, W., Yao, M.[2015]: Study of hidden attractors, multiple limit cycles from Hopf bifurcation and boundedness of motion in the generalized hyperchaotic Rabinovich system. Nonlinear Dynamics **82**(1) 131–141

Danca, M.F., Kuznetsov, N., Chen, G.[2017]: Unusual dynamics and hidden attractors of the Rabinovich–Fabrikant system. Nonlinear Dynamics **88** 791–805

Jafari, S., Pham, V.T., Golpayegani, S., Moghtadaei, M., Kingni, S.[2016]: The relationship between chaotic maps and some chaotic systems with hidden attractors. Int. J. Bifurcat. Chaos **26**(13) art. num. 1650211.

Menacer, T., Lozi, R., Chua, L.[2016]: Hidden bifurcations in the multispiral Chua attractor. International Journal of Bifurcation and Chaos **26**(14) art. num. 1630039.

Ojoniyi, O., Njah, A.[2016]: A 5D hyperchaotic Sprott B system with coexisting hidden attractors. Chaos, Solitons & Fractals **87** 172–181

Pham, V.T., Volos, C., Jafari, S., Vaidyanathan, S., Kapitaniak, T., Wang, X.[2016]: A chaotic system with different families of hidden attractors. International Journal of Bifurcation and Chaos **26**(08) 1650139

Rocha, R., Medrano-T, R.O.[2016]: Finding hidden oscillations in the operation of nonlinear electronic circuits. Electronics Letters **52**(12) 1010–1011

Wei, Z., Pham, V.T., Kapitaniak, T., Wang, Z.[2016]: Bifurcation analysis and circuit realization for multiple-delayed Wang–Chen system with hidden chaotic attractors. Nonlinear Dynamics **85**(3) 1635–1650

Zelinka, I.[2016]: Evolutionary identification of hidden chaotic attractors. Engineering Applications of Artificial Intelligence **50** 159–167

Borah, M., Roy, B.: Hidden attractor dynamics of a novel non-equilibrium fractional-order chaotic system and its synchronisation control. In: 2017 Indian Control Conference (ICC). 450–455

Feng, Y., Pan, W.[2017]: Hidden attractors without equilibrium and adaptive reduced-order function projective synchronization from hyperchaotic Rikitake system. Pramana **88**(4) 62

Jiang, H., Liu, Y., Wei, Z., Zhang, L.[2016]: Hidden chaotic attractors in a class of two-dimensional maps. Nonlinear Dynamics **85**(4) 2719–2727

Kuznetsov, N., Leonov, G., Yuldashev, M., Yuldashev, R.[2017]: Hidden attractors in dynamical models

of phase-locked loop circuits: limitations of simulation in MATLAB and SPICE. Commun Nonlinear Sci Numer Simulat **51** 39–49

Ma, J., Wu, F., Jin, W., Zhou, P., Hayat, T.[2017]: Calculation of Hamilton energy and control of dynamical systems with different types of attractors. Chaos: An Interdisciplinary Journal of Nonlinear Science **27**(5) 053108

Messias, M., Reinol, A.[2017]: On the formation of hidden chaotic attractors and nested invariant tori in the Sprott A system. Nonlinear Dynamics **88**(2) 807–821

Rabinovich, M.I. & Fabrikant, A.L. [1979] "Stochastic self-modulation of waves in nonequilibrium media," *J. Exp. Theor. Phys.* **77**, 617–629.

Danca, M.-F.[2016) "Hidden transient chaotic attractors of Rabinovich-Fabrikant system," Nonlinear Dynamics, 86(2), 12631270.

Molaie, M., Jafari, S., Sprott, J.C., Golpayegani, S.M.R.H. [2013] "Simple chaotic flows with one stable equilibrium," *Int. J. Bifurcation and Chaos* **23**, 1350188.

Singh, J., Roy, B.[2017]: Multistability and hidden chaotic attractors in a new simple 4-D chaotic system with chaotic 2-torus behaviour. International Journal of Dynamics and Control https://doi.org/10.1007/s40435-017-0332-8.

Volos, C., Pham, V.T., Zambrano-Serrano, E., Munoz-Pacheco, J.M., Vaidyanathan, S., Tlelo-Cuautle, E.[2017]: Analysis of a 4-D hyperchaotic fractional-order memristive system with hidden attractors. In: Advances in Memristors, Memristive Devices and Systems. Springer 207–235

Wei, Z., Moroz, I., Sprott, J., Akgul, A., Zhang, W.[2017]: Hidden hyperchaos and electronic circuit application in a 5D self-exciting homopolar disc dynamo. Chaos **27**(3) art. num. 033101.

Zhang, G., Wu, F., Wang, C., Ma, J.[2017]: Synchronization behaviors of coupled systems composed of hidden attractors. International Journal of Modern Physics B **31** art. num. 1750180.

Grebogi, C., Ott, E., Yorke, J.A. [1983] Fractal basin boundaries, long-lived chaotic transients, and unstable-unstable pair bifurcation. Phys. Rev. Lett. 50, 935938

Brenan KE, Campbell SL, Petzold LR. [1996]Numerical Solution of Initial-Value Problems in Differential-Algebraic Equations (SIAM Classics in Applied Mathematics, 14). SIAM: Philadelphia; 1996.

S.A. Sarra and C. Meador[2011]. On the numerical solution of chaotic dynamical systems using extend precision floating point arithmetic and very high order numerical methods. Nonlinear Analysis: Modelling and Control , 16(3):340352

P. Wang, J. Li, and Q. Li. [2012] Computational uncertainty and the application of a high-performance multiple precision scheme to obtaining the correct reference solution of Lorenz equations. Numerical Algorithms, 59(1):147159, 2012

N.V. Kuznetsov, G.A. Leonov, T.N. Mokaev, Finite-time and exact Lyapunov diension of the Henon map, https://arxiv.org/abs/1712.01270, 2017

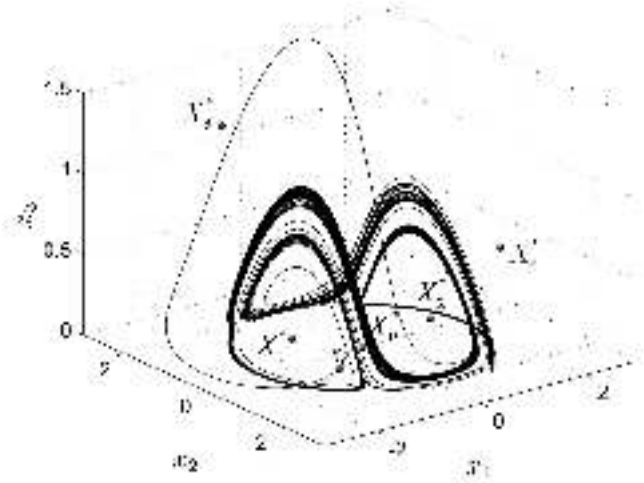

Fig. 1. Hidden chaotic attractor of the system RF (1) for $a = 0.1$ and $b = 0.2876$. $X^*_{1,2}$ are stable equilibria, while $X_{0,3,4}$ are unstable equilibria.

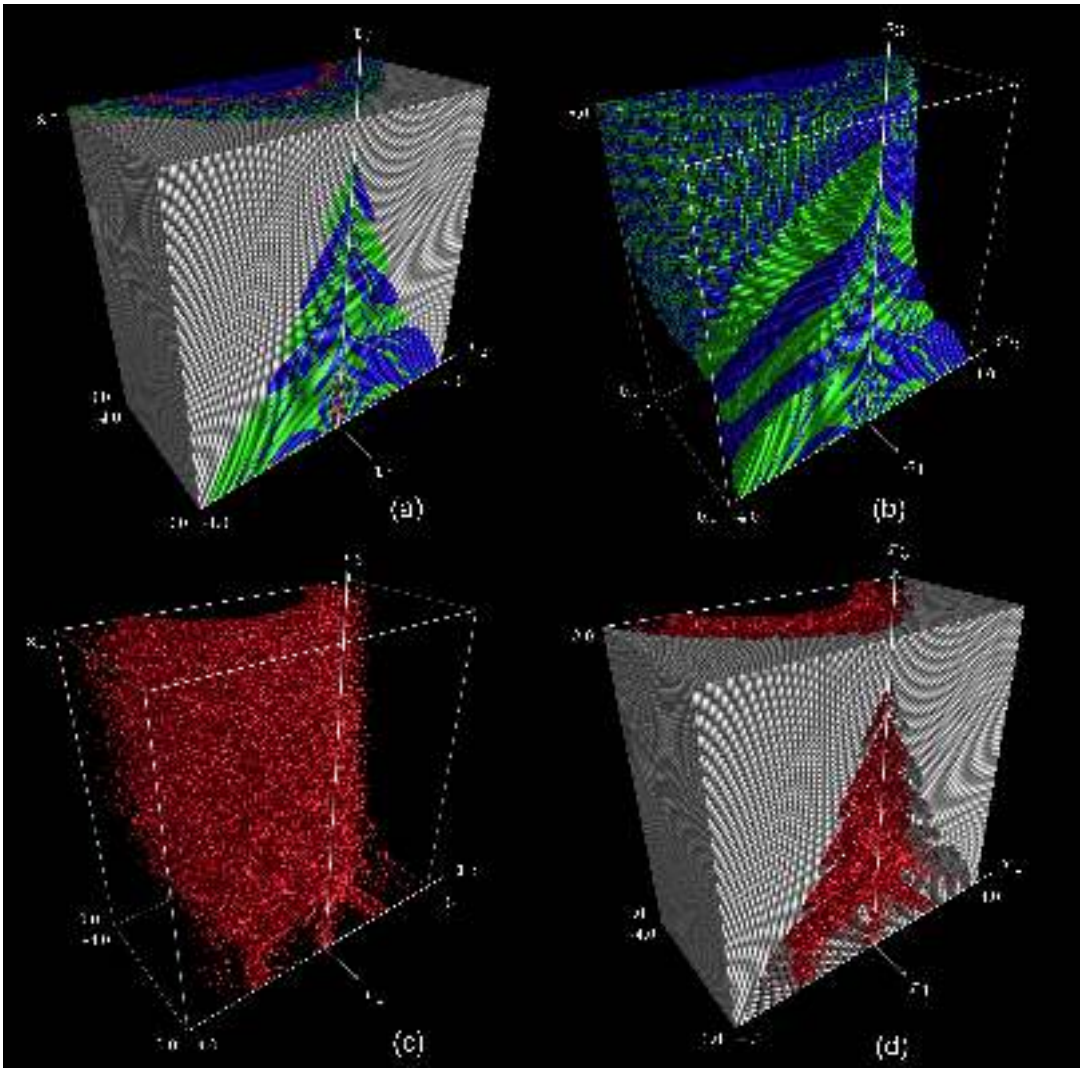


Fig. 2. (a) A relatively large view of attraction basins. (b) Attraction basins of the stable equilibria $X^*_{1,2}$; (c) Attraction basin of the hidden chaotic attractor $H$; (d) Attraction basin of the hidden chaotic attractor $H$ together with divergence points.

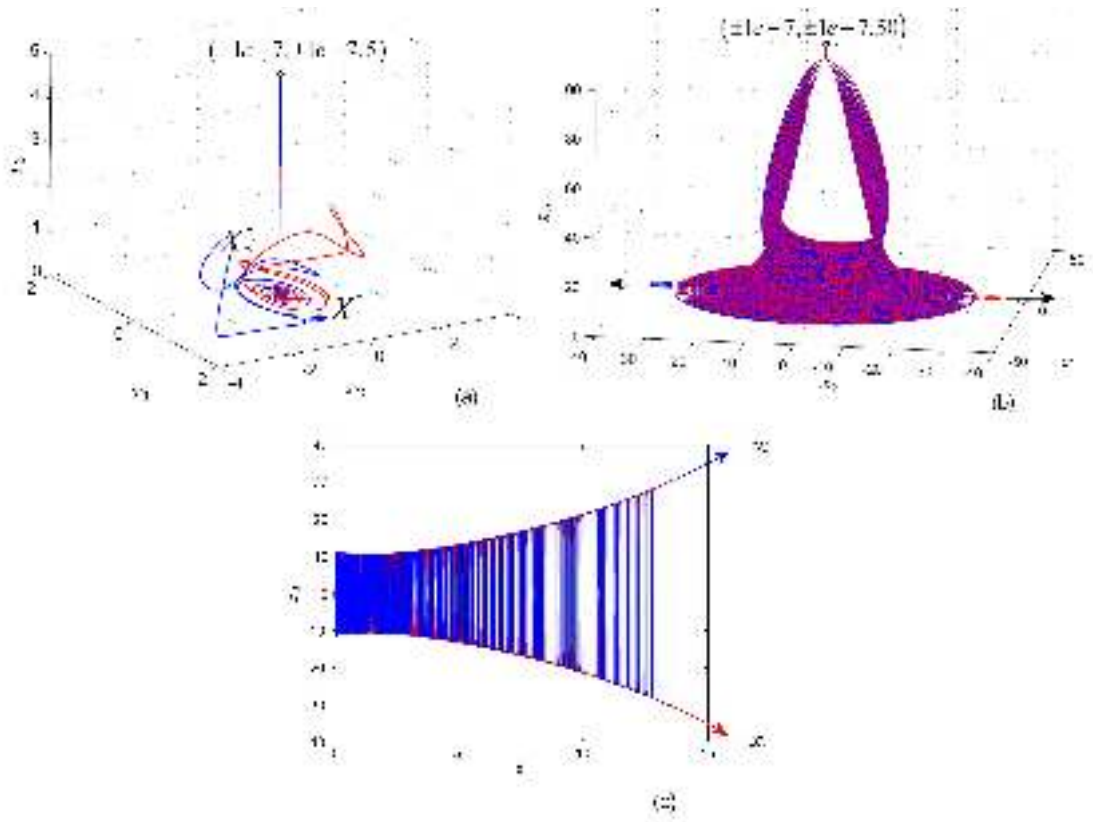

Fig. 3. Superimposed trajectories for the same parameters $a = 0.1$ and $b = 0.2876$, but for different initial conditions. (a) Initial conditions $x_0 = (1e-7, 1e-7, 5)$ and $x_0 = (-1e-7, -1e-7, 5)$; (b) Initial conditions $x_0 = (1e-7, 1e-7, 50)$ and $x_0 = (-1e-7, -1e-7, 50)$. (c) Time series $(x_2)$ shows that there exist unstable transient oscillations, before the trajectories diverge.

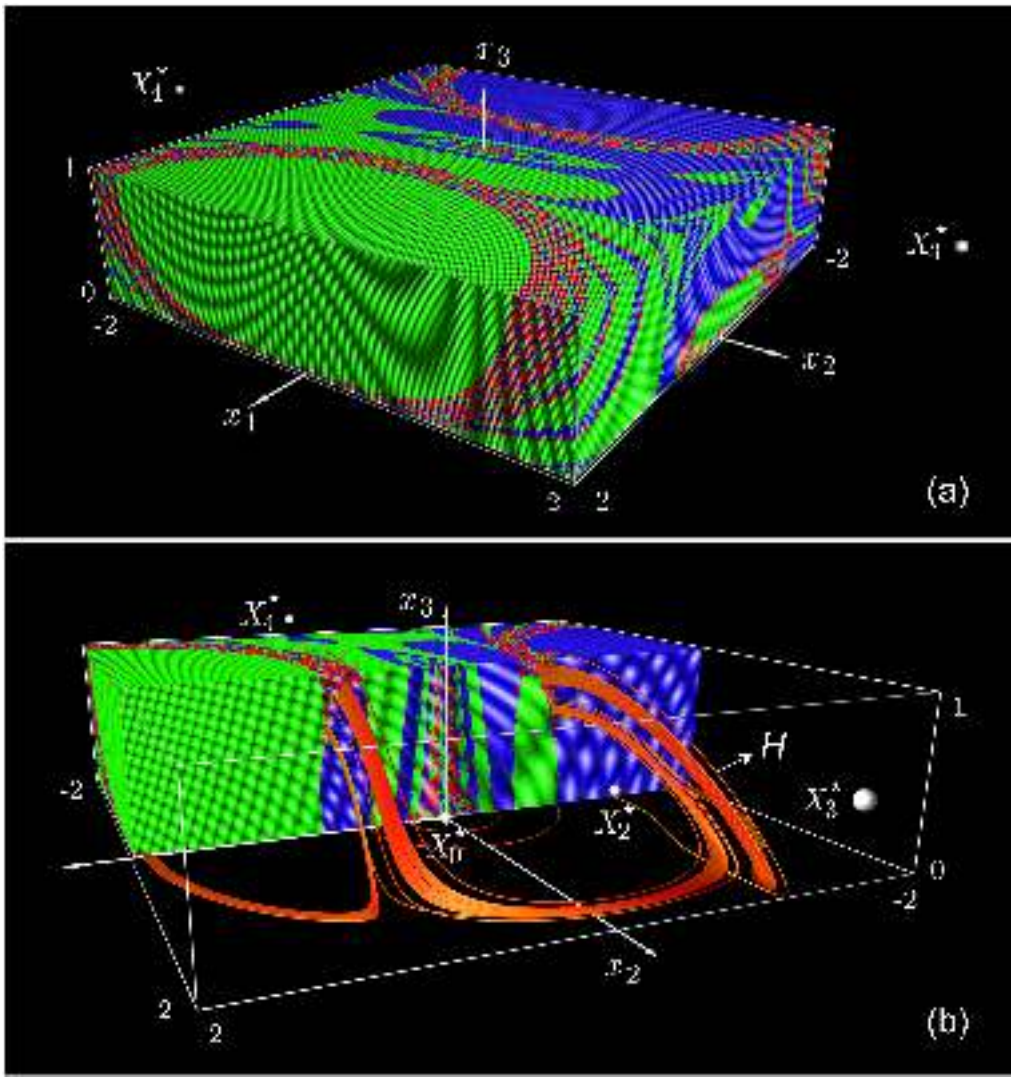


Fig. 4. Parallelepiped neighborhood of the unstable equilibrium $X_0^*$. Blue points represent the initial conditions which lead to the stable equilibrium $X_1^*$, green points lead to the stable equilibrium $X_2^*$, while the red points lead to the hidden attractor $H$; (a) General view; (b) Hidden attractor overplotted on the parallelipipedic neighborhood.

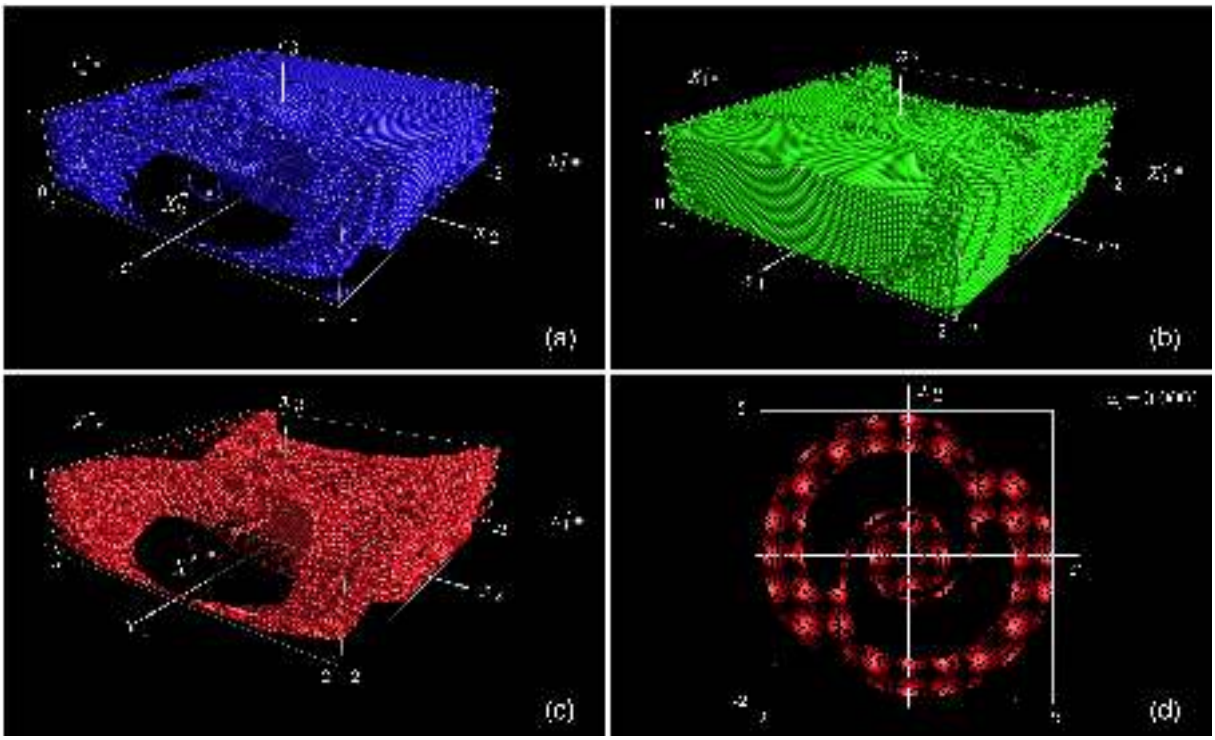


Fig. 5. Separate views of partial attraction basins; (a) Points of the attraction basins of the stable equilibrium $X_1^*$ (not visible here); Points of the attraction basins of the stable equilibrium $X_2^*$ (not visible here); (c) Points of the attraction basins of the hidden attractor $H$; (d) Section through the attraction basin in Fig. 5 (c) with the plane $x_3 = 0.0001$.

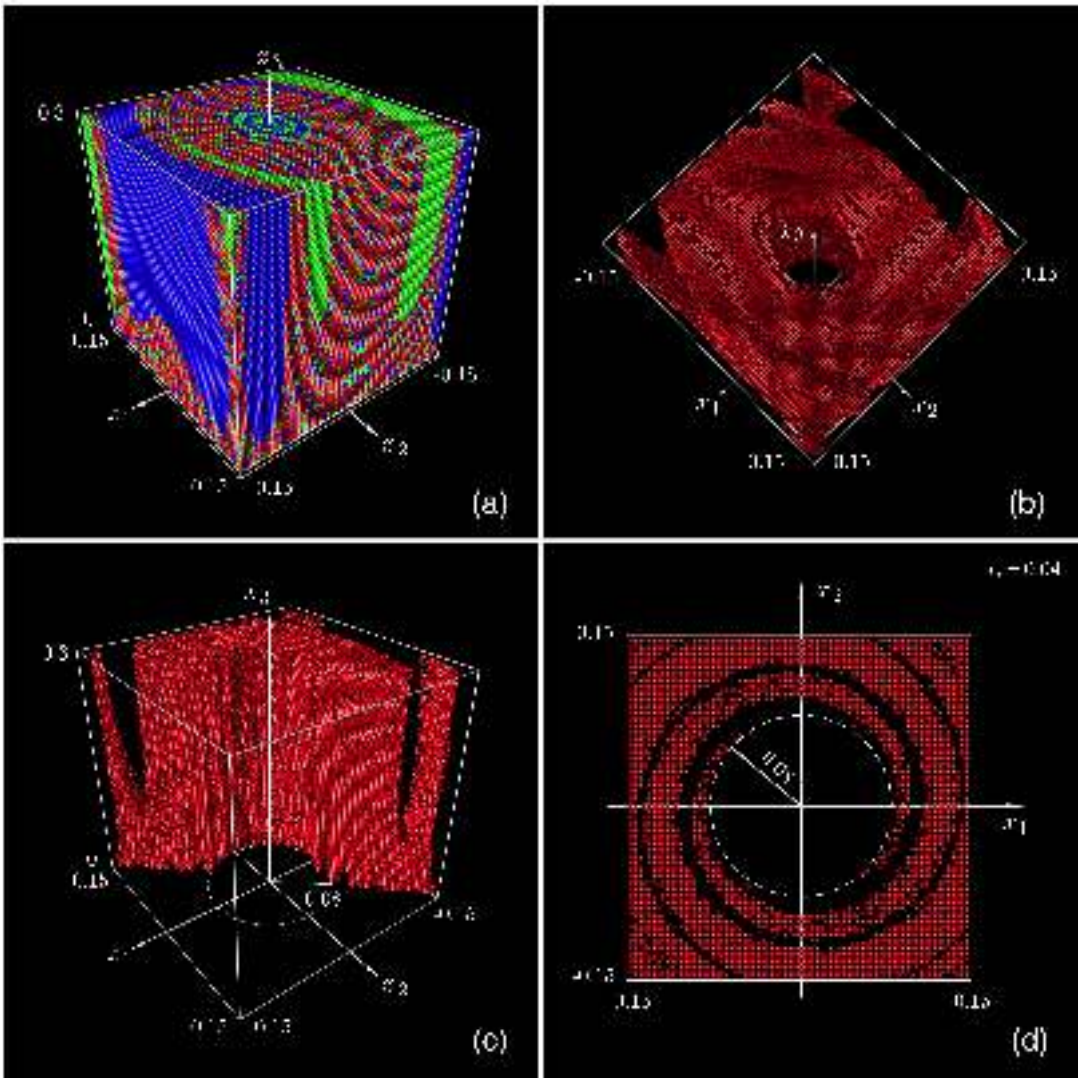


Fig. 6. Zoomed detail of the parallelipiped in Fig. 4 (a), containing the unstable equilibrium $X_0^*$; (a) General view, revealing the possible fractal structure of the basins boundaries; (b) View of the initial points leading to the hidden attractor $H$ unveiling the empty space around the unstable point $X_0^*$; (c) Vertical section through the attraction basin of $H$ in Fig. 6 (b) presenting the cylinder-like shape of the empty region, of ray 0.08; (d) Horizontal section with the plane $x_3 = 0.04$.

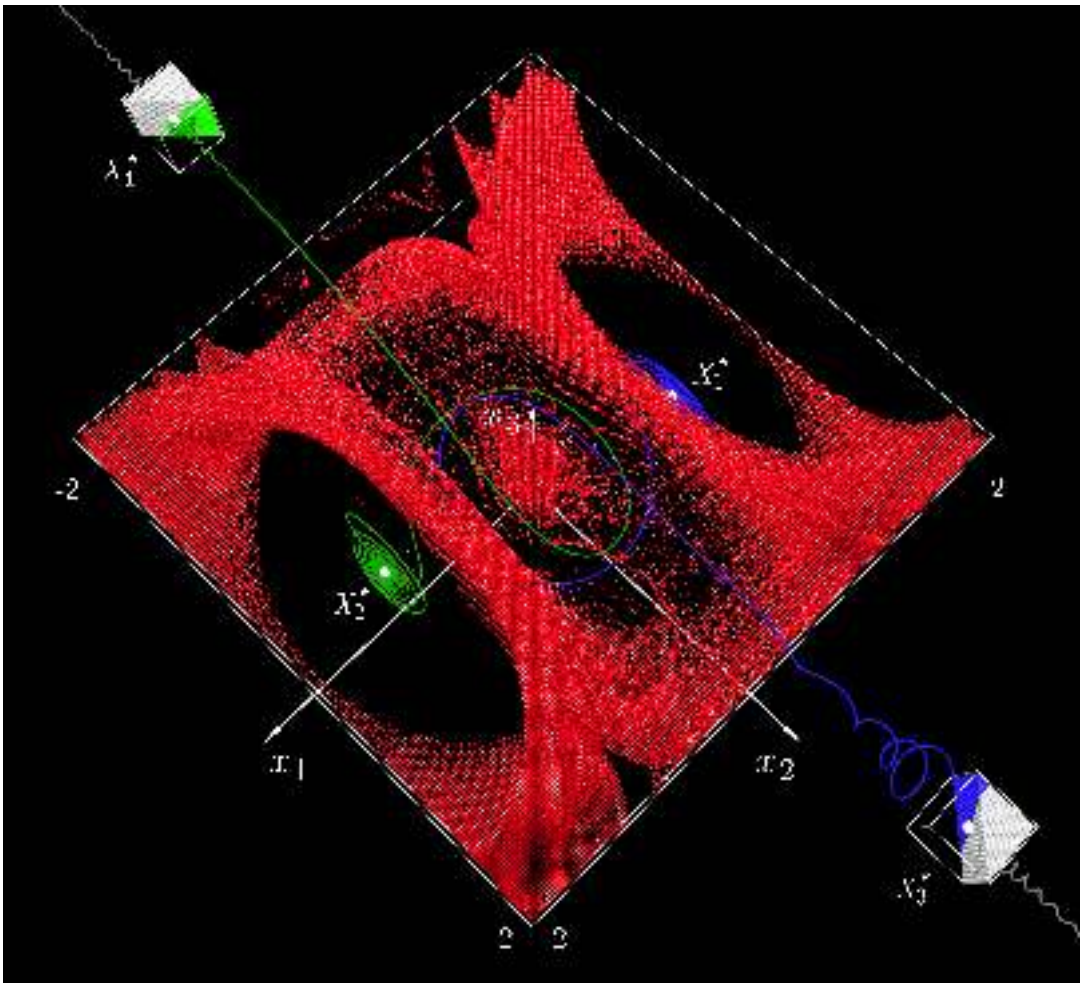


Fig. 7. General view of all equilibria and their partial attraction basins. From any points in the neighborhoods of the unstable equilibria $X^*_{3,4}$ the trajectories tend either to the stable equilibrium $X^*_1$ (blue), or to the stable equilibrium $X^*_2$ (green), or diverge (gray). Attraction basins of $X^*_{1,2}$ are not drawn here.